Journal of Biomedical Optics

BiomedicalOptics.SPIEDigitalLibrary.org

Evaluation of the usefulness of three-dimensional optical coherence tomography in a guinea pig model of endolymphatic hydrops induced by surgical obliteration of the endolymphatic duct

Nam Hyun Cho
Jang Woo Lee
Jin-ho Cho
Jeehyun Kim
Jeong Hun Jang
Woonggyu Jung

SPIE.

Evaluation of the usefulness of three-dimensional optical coherence tomography in a guinea pig model of endolymphatic hydrops induced by surgical obliteration of the endolymphatic duct

Nam Hyun Cho,[a,b] Jang Woo Lee,[a] Jin-ho Cho,[a] Jeehyun Kim,[a] Jeong Hun Jang,[c,*] and Woonggyu Jung[b,d,*]
[a]Kyungpook National University, School of Electronics Engineering, 1370 Sankyuk 3-dong, Buk-gu, Daegu 702-701, Republic of Korea
[b]Institute for Basic Science, Center for Soft and Living Matter, Banyeon-ri, Eonyang-eup, Ulju-gun, Ulsan 689-798, Republic of Korea
[c]Kyungpook National University College of Medicine, Department of Otorhinolaryngology, 680 Gukchaebosang-ro, Jung-gu, Daegu 700-842, Republic of Korea
[d]Ulsan National Institute of Science and Technology, School of Nano-Bioscience and Chemical Engineering, 689-798, Republic of Korea

Abstract. Optical coherence tomography (OCT) has advanced significantly over the past two decades and is currently used extensively to monitor the internal structures of organs, particularly in ophthalmology and dermatology. We used ethylenediamine tetra-acetic acid (EDTA) to decalcify the bony walls of the cochlea and investigated the inner structures by deep penetration of light into the cochlear tissue using OCT on a guinea pig model of endolymphatic hydrops (EH), induced by surgical obliteration of the endolymphatic duct. The structural and functional changes associated with EH were identified using OCT and auditory brainstem response tests, respectively. We also evaluated structural alterations in the cochlea using three-dimensional reconstruction of the OCT images, which clearly showed physical changes in the cochlear structures. Furthermore, we found significant anatomical variations in the EH model and conducted graphical analysis by strial atrophy for comparison. The physical changes included damage to and flattening of the organ of Corti—evidence of Reissner's membrane distention—and thinning of the lateral wall. These results indicate that observation of EDTA-decalcified cochlea using OCT is significant in examination of gradual changes in the cochlear structures that are otherwise not depicted by hematoxylin and eosin staining. [DOI: 10.1117/1.JBO.20.3.036009]

Keywords: optical coherence tomography; cochlea; endolymphatic hydrops; Reissner's membrane; auditory brainstem response; ethylenediamine tetra-acetic acid.

Paper 140864R received Dec. 28, 2014; accepted for publication Feb. 19, 2015; published online Mar. 12, 2015.

1 Introduction

This paper reports on direct clinical studies conducted using optical coherence tomography (OCT) as a noninvasive imaging tool to visualize the internal structures of the cochlea. The axial and spatial resolutions of OCT are both in the range of 1 to 10 μm and the penetration depth is in the range of 2 to 10 mm, depending on the translucency of the sample tissue. Micro electro mechanical systems-vertical cavity surface emitting laser laser-based ultrahigh speed swept source-OCT is also being actively developed.[1,2] By virtue of these characteristics, OCT is clinically used in the fields of ophthalmology and dermatology to visualize the eye and superficial layers of the skin.[3,4] Further, OCT has been applied in imaging of the laryngeal mucosa;[5] thus, it can also be utilized in the field of otorhinolaryngology. However, clinical application of OCT in imaging of inner ear structures such as the cochlea is limited because of its relatively shallow penetration depth and the presence of bony walls. As a result, previous studies on cochlear imaging using OCT have shown only very limited regions.[6–8]

In a previous study, we demonstrated the *in vivo* imaging of mouse cochlea using spectral domain OCT combined with a surgical microscope.[9] In that study, the tympanic membrane—middle ear structures, including the ossicles—and cochlea were visualized through a transtympanic view and three-dimensional (3-D) OCT images were acquired. Kakigi et al. evaluated the internal structure of guinea pig cochlea using OCT.[10] In their study, the harvested cochlea were decalcified by immersion in ethylenediamine tetra-acetic acid (EDTA) for 14 days, then its internal structures were extracted and clearly visualized using OCT. The study suggested that the utility of OCT was comparable with that of hematoxylin and eosin (H&E) staining and that OCT images in arbitrary planes can be obtained by manipulating the slice axis of the specimens.

Meniere's disease is an inner ear disorder that is clinically characterized by recurrent vertigo, fluctuating hearing loss, tinnitus, and ear fullness. Endolymphatic hydrops (EH) is a typical histologic finding that is commonly detected in specimens from patients with Meniere's disease. It is difficult to identify EH in patients with Meniere's disease because clinical examinations such as the auditory brainstem response (ABR) and caloric tests only provide functional information regarding a damaged cochlea or vestibule. Consequently, many studies have attempted to investigate the pathophysiology of Meniere's disease and

*Address all correspondence to: Woonggyu Jung, E-mail: wgjung@unist.ac.kr; Jeong Hun Jang, E-mail: jangjh@knu.ac.kr

the presence/absence of EH using histological examination in animal models,[11–17] with the most popular model being that induced by surgical ablation of the endolymphatic duct and sac. A surgical technique proposed by Kimura requires penetration of the brain's protective covering, leading to an increase in morbidity and mortality associated with penetration of the central nervous system. To prevent this complication, Andrews and Bohmer developed an extradural approach which was subsequently revised by Megerian et al.[18] Our current study is designed to clearly visualize the internal structures of the cochlea using 3-D OCT after EDTA-induced decalcification of the bony walls in a guinea pig model of surgically induced EH.

2 Materials and Methods

2.1 *OCT System*

Figure 1 is a schematic of the SD-OCT system developed. The system comprises a 2048-pixel, 12-bit complementary metal-oxide semiconductor line-scan camera (Sprint spL2048-140k, Basler AG, Germany) with a 70,000 line/s effective line rate. A transmission-type diffraction grating (spatial frequency, 1800 lpmm; nominal AOI/AOD, 46.05 deg; Wasatch Photonics) was implemented to enhance the light detection efficiency in the path. A fiber-based interferometer was equipped with the junction of a superluminescent light-emitting diode as the light source. The center wavelength of the source was 870 nm with a bandwidth of 65 nm, thus yielding an axial resolution of 6 μm and a lateral resolution of 10 μm. The light beam from the source passed through the optical component of the beam splitter such that one-half of the light beam was in the sample and the other half was directed toward the reference arms. We used the reference arm for cochlea imaging as it also contained a dispersion compensation unit (prism pair) to account for the dispersion within the optics of the sample path.[19] Reflected light from the static mirror in the reference arm combined with back-scattered light from different depths in the sample at the beam splitter. B-mode scanning was performed using a galvanometer scanning mirror in the rear focal plane of the objective lens in the sample arm. A double aspheric lens (30 D; image magnify, 2.15×; Volk) was used to minimize the aberration and dispersion of the lenses. We used an objective lens with a 30 mm focal length to deliver a beam of 2-mm diameter onto the cochlea. The output from the line camera was connected to a computer through a frame grabber (PCIe-1433, 850-MB/s bandwidth, National Instruments). The galvanometer scanning mirror was driven by the computer through a data acquisition board (PCIe-6321, National Instruments).

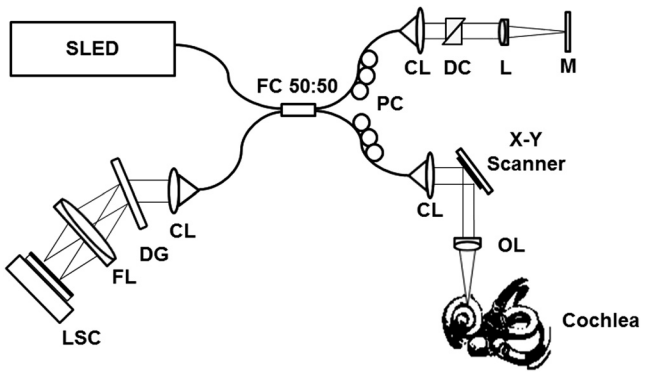

Fig. 1 Schematic diagram of the spectral domain optical coherence tomography (OCT) system. Abbreviations: SLED, superluminescence diode; FC, fiber coupler; PC, polarization controllers; CL, collimator; DC, dispersion compensation unit (prism pair); L, lens; M, mirror; DG, diffraction grating; FL, focusing lens; LSC, line-scan camera; and OL, objective lens.

2.2 *Model Preparation and OCT Observations*

The animal experiments were conducted in accordance with the guidelines of the Institutional Animal Care and Use Committee of Kyungpook National University. A 5-week-old guinea pig (Slc: Hatley strain) weighing approximately 180 g was used in this study. The animal was anesthetized by intramuscular injection of a mixture of tiletamine/zolazepam (1.8 mg/100 g) and xylazine hydrochloride (0.7 mg/100 g). After local injection of 2% lidocaine HCI and epinephrine (1 : 100,000), a postauricular skin incision was made. Figure 2(a) shows the surgical obliteration of the endolymphatic duct procedure. For the surgical induction of EH,[20] the animal was placed in the prone position using a head holder, and a dorsal midline scalp incision was made under a surgical microscope. After making a horizontal incision along the neck muscle to expose the bony occiput, the temporo-occipital suture was exposed. The bone in the area inferior and lateral to the suture was then drilled. Following identification of the sigmoid sinus, the bone overlying the sinus was removed using a pick. The sigmoid sinus was then medially retracted to expose the operculum. A 0.5-mm burr was used to drill from the medial to the operculum and into the endolymphatic sac and duct. The endolymphatic duct was then packed with bone wax using a straight pick. The skull defect was reinforced with Gelfoam (Pfizer, New York). The muscles were sutured together using 4-0 POLYSORB (United States Surgical, Norwalk, Connecticut) sutures. The surgical

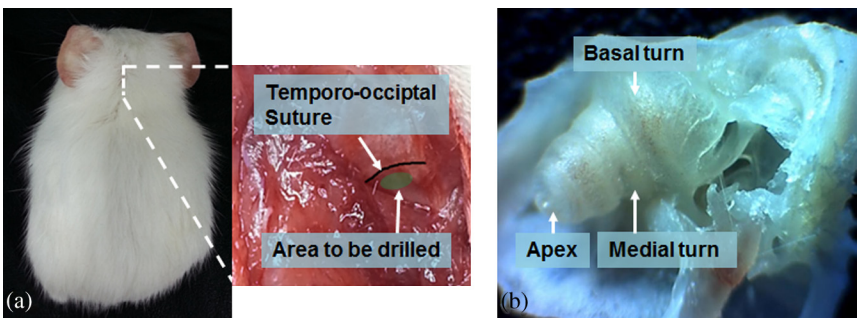

Fig. 2 (a) Surgical obliteration of the endolymphatic duct procedure and (b) microscope image of the cochlea of the *ex vivo* guinea pig.

procedure was performed in both ears with a 1-week interval between procedures. Figure 2(b) shows the entire cochlea of the *ex vivo* guinea pig. For EDTA solution of OCT observations,[21] both temporal bones were obtained immediately after fixation and stored in 10% formalin solution for 1 week. Subsequently, the specimens were decalcified by immersion in EDTA for 14 days.

3 Results

Figure 3(a) shows the results of open field-based ABRs recorded in a soundproof booth at 2 kHz pure tone stimuli. The postoperative ABR was measured using a commercial auditory workstation system (Tucker-Davis Technologies) comprising RZ6 (multi-I/O processor), RA 4PA (medusa preamp), RA 4LI (low-impedance headstage), MF 1 (magnetic speaker), BioSigRZ (measurement software), and PO5e (PC interface card). An ABR recording was used to monitor the auditory function of the experimental animal. Under general anesthesia, subdermal needle electrodes were inserted ventrolateral to the measured ear (i: active), contralateral to the measured ear (ii, iii: reference), and into the vertex (iv: ground). The acoustic stimuli and ABR recordings consisted of pure tones at 2, 4, 8, and 16 kHz. Figures 3(b)–3(f) show the results of ABR testing at 2 kHz. Similar results were observed at 4, 8, and 16 kHz. Figure 3(b) shows the preoperative ABR for the left ear (control); the threshold was 45 dB HL. The (1), (2), (3), and (4) peaks appear clear and sharp. Figure 3(c) shows the ABR for the left ear 1 week after surgery; the threshold was 55 dB HL. Compared with that in Fig. 3(b), the hearing level was attenuated by approximately 10 dB HL. Analysis of the (2) and (4) peaks confirmed that the hearing level after surgery was slightly attenuated compared with that before surgery. Figure 3(d) shows the ABR for the right ear (control), which shows a threshold of 45 dB HL, similar to that for the left ear. Figure 3(e) shows the ABR for the right ear 1 week after surgery, with a threshold similar to that in Fig. 3(c). Figure 3(f) shows the ABR for the right ear 2 weeks after surgery, which was unable to measure the threshold at 55 dB HL. The amplitude of the ABR peaks (arrow heads) after surgery in the left ear [(b) and (c)] and right ear [(d)–(f)] are decreasing, as shown by the white dotted line (55 dB HL). The ABR test results confirmed the presence of a hearing deficiency when the thresholds reached approximately 70 dB HL. The ABR test results shown in Fig. 3 confirm that EH surgery was successful.

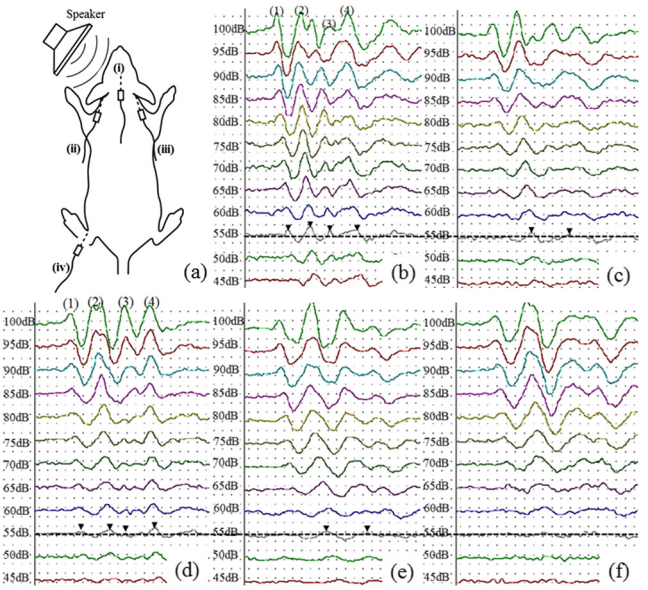

Fig. 3 Auditory brainstem response (ABR) thresholds of 2 kHz pure tone stimuli: (a) open space based ABR recoding (i) active (+), (ii) left reference (–), (iii) right reference (–), (iv) ground; (b) preoperative ABR of left ear; (c) postoperative 1-week ABR of left ear; (d) preoperative ABR of right ear; (e) postoperative 1-week ABR of right ear; and (f) postoperative 2-week ABR of right ear. The amplitude of the ABR peaks (arrow heads) after surgery in the [(b) and (c)] left and [(d)–(f)] right ears is decreasing, as shown by the white dotted line (55 dB HL).

Figure 4 shows the two-dimensional (2-D)/3-D cross-sectional OCT images of the internal structures of an intact cochlea. The bony labyrinth exhibits a spiral shape, similar to the space inside the shell of a snail. The cochlea comprises relatively large fluid-filled spaces: the scala vestibuli, media, and tympani. Furthermore, a wide variety of tissue types, ranging from acellular gelatinous material (Reissner's membrane), to dense bone, to the epithelial organ of Corti which contains remarkably delicate hair cells, can be visualized. Compared to 2-D OCT, 3-D OCT imaging can be used to confirm the overall volume of the cochlea structure and disease volume. In addition, it facilitates analysis of the structural features in various locations and angles. Figures 4(a) and 4(b) show the 2-D/3-D images of the internal structures of a normal cochlea. The scala vestibuli, media, and tympani are distinct. Figure 4(b) verifies each respective structure in a symmetrical fashion. Figures 4(c) and 4(d) show the 2-D/3-D images of the internal structures in the 1 week postsurgical EH model. Unlike that in the basal turn, the bulging Reissner's membrane in the apical turn is bent into the scala vestibuli. This was accurately confirmed on a 3-D-reconstructed image of Fig. 4(d); the bulging Reissner's membrane in the basal

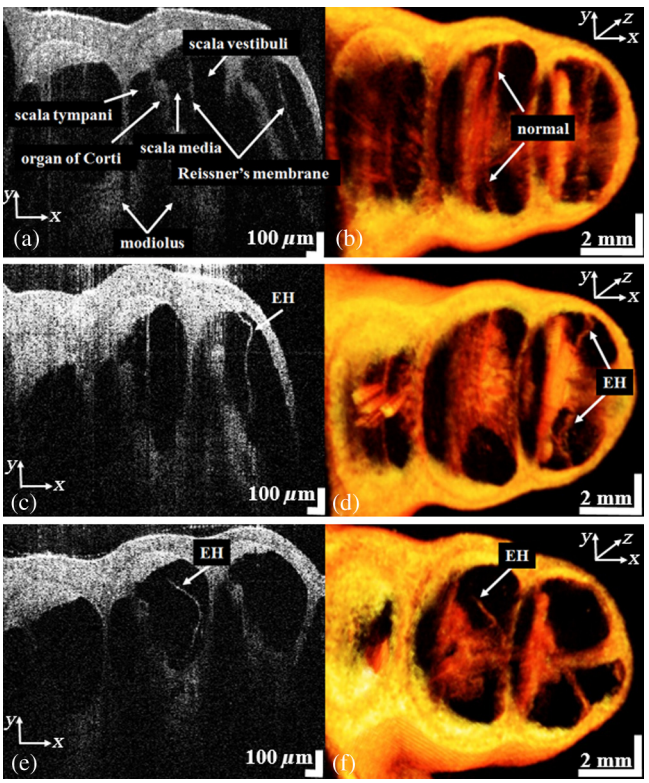

Fig. 4 Two-dimensional/three-dimensional OCT images of the cochlea of an *ex vivo* guinea pig: (a) and (b) normal; (c) and (d) left cochlea 1 week after surgery; (e) and (f) right cochlea 2 weeks after surgery.

turn was also found to bend into the scala vestibuli. More detailed information for the same region is provided in Fig. 4(f).

Figures 3(b), 3(d), and 3(f), which start from the right, are en-face images of the apex, medial turn, and basal turn from the 3-D cochlea image. Each of the inner cochlea structures can be clearly identified in the images. Moreover, we can get an understanding of the volume of the scala tympani, scala media, and scala vestibule and the structure of the organ of Corti and modiolus from the 3-D OCT images. In addition, the morphological features of the Reissner's membrane, which is affected by EH, are clearly shown in the 3-D OCT images, in contrast to those in the 2-D OCT images. The imaging window of the entire cochlea of the guinea pig was approximately 3 mm × 2 mm. Therefore, 1024 × 500 pixels were required to cover the imaging window in the high speed LabVIEW-based system, which allows 56 fps for real-time display. For the 3-D OCT data, approximately 5 s was required to acquire 1024 × 500 × 500 pixels of the 3-D OCT image in the same system. In this paper, the high speed OCT system facilitated analysis of the structural variations at the inner cochlea from the 3-D OCT image of the cochlea of the guinea pig.

4 Discussion

Since OCT images of a rat cochlea were reported,[22] many studies evaluating the cochlea using OCT have been conducted. Sepehr et al. visualized porcine cochlea through OCT.[8] Instead of decalcification, they thinned the bone from the basal turn of the cochlea, keeping the endosteum intact. Gao et al. quantitatively analyzed the soft tissue of the cochlear using wild-type and *Tecta* transgenic mice *in vitro*.[23] In addition, the superiority of OCT over conventional histology was indicated by the SD-OCT detection of anatomical changes in the organ of Corti during postnatal cochlear development. In that study, the apical bone in the otic capsule was removed to minimize unwanted scattering. Tona et al. reported that OCT is useful for the evaluation of EH using *Slc26A4*$^{(-/-)}$ mice *in vivo*.[17] In that study, the second turn was chosen to estimate EH because of the limited penetration depth of OCT. The hearing level was estimated and OCT images and histological findings were compared in *Slc26A4*$^{(-/-)}$, *Slc26A4*$^{(+/-)}$, and *Slc26A4*$^{(+/+)}$ mice. Kakigi et al. visualized the cochlea of a guinea pig using OCT. The feasibility of OCT for quantitative assessment of the endolymphatic space, organ of Corti, and lateral wall was evaluated by comparison with H&E-stained images using a surgically induced EH model,[11] a model of deafness induced by kanamycin-ethacrynic acid,[24] and a model of strial atrophy induced by streptomycin sulfate perfusion.[25] Unlike the procedure utilized in the study by Tona et al.,[17] in this study, cochlear OCT images were acquired *in vitro* after decalcification using EDTA to achieve a high resolution. In the current study, 3-D reconstruction of the OCT images was performed and the hearing status was evaluated at different time points after surgical induction of EH. Hearing loss is one of the essential symptoms of Meniere's disease. Destructive change by recurrent distension of Reissner's membrane causes aggravation of hearing status; hence, the extent of EH is related to the hearing level. In this study, the ABR thresholds of the right ear increased at serial measurement postoperatively, which indirectly supports the correlation between pathologic change and hearing change. These procedures were not included in the above-mentioned studies.

One limitation of this study is that pathologic analysis was not conducted. However, abnormal OCT findings in EH, such as Reissner's membrane distension, were confirmed by comparison with pathologic analyses in previous studies,[9,16] and the abnormal findings of OCT images in this study were consistent with those of previous studies. Both 2-D and 3-D OCT images clearly showed the abnormal EH findings, indicating the potential of OCT as an effective tool for analyzing cochlear pathologies. Although light scattering by bony structures can be a potential limitation in further studies, various advantages of OCT in the field of otology will help to overcome this limitation.

5 Conclusions

In this study, we decalcified the bony walls of the cochlea using EDTA solution and clearly and widely visualized the internal structures of the cochlea of a guinea pig model of EH induced by surgical obliteration of the endolymphatic duct using OCT. Our findings demonstrate that imaging of the decalcified cochlea using OCT is of significant value in the examination of cochlear pathology, particularly EH, before or without histological examination. Studies comparing histological examination using H&E staining with 2-D/3-D OCT are under way.

Acknowledgments

This work was financially supported by a grant from the National Institutes of Health (No. 201225940000), "Development of Micro-surgical Apparatus based on 3-D Tomographic Operating Microscope," funded by the Ministry of Trade, Industry, and Energy (MI, Korea) (No. 10047943), and Project Code (IBS-R020-D1).

References

1. I. Grulkowski et al., "Retinal, anterior segment and full eye imaging using ultrahigh speed swept source OCT with vertical-cavity surface emitting lasers," *Biomed. Opt. Express* **3**(11), 2733–2751 (2012).
2. I. Grulkowski et al., "High-precision, high-accuracy ultralong-range swept-source optical coherence tomography using vertical cavity surface emitting laser light source," *Opt. Lett.* **38**(5), 673–675 (2013).
3. J. A. Izatt et al., "Micrometer-scale resolution imaging of the anterior eye in vivo with optical coherence tomography," *Arch. Ophthalmol.* **112**(12), 1584–1589 (1994).
4. J. Welzel, "Optical coherence tomography in dermatology: a review," *Skin Res. Technol.* **7**(1), 1–9 (2001).
5. A. G. Bibas et al., "3-D optical coherence tomography of the laryngeal mucosa," *Clin. Otolaryngol. Allied Sci.* **29**(6), 713–720 (2004).
6. B. J. Wong et al., "Imaging the internal structure of the rat cochlea using optical coherence tomography at 0.827 microm and 1.3 microm," *Otolaryngol. Head Neck Surg.* **130**(3), 334–338 (2004).
7. J. Lin, H. Staecker, and M. S. Jafri, "Optical coherence tomography imaging of the inner ear: a feasibility study with implications for cochlear implantation," *Ann. Otol. Rhinol. Laryngol.* **117**(5), 341–346 (2008).
8. A. Sepehr et al., "Optical coherence tomography of the cochlea in the porcine model," *Laryngoscope* **118**(8), 1449–1451 (2008).
9. N. H. Cho et al., "In vivo imaging of middle-ear and inner-ear microstructures of a mouse guided by SD-OCT combined with a surgical microscope," *Opt. Express* **22**(8), 8985–8995 (2014).
10. A. Kakigi et al., "Evaluation of the internal structure of normal and pathological guinea pig cochleae using optical coherence tomography," *Audiol. Neurotol.* **18**(5), 335–343 (2013).
11. R. S. Kimura, "Experimental blockage of the endolymphatic duct and sac and its effect on the inner ear of the guinea pig: a study on endolymphatic hydrops," *Ann. Otol. Rhinol. Laryngol.* **76**(3), 664–687 (1967).
12. J. C. Andrews and A. Bohmer, "The surgical approach to the endolymphatic sac and the cochlear aqueduct in the guinea pig," *Am. J. Otolaryngol.* **10**(1), 61–66 (1989).

13. C. H. Kim et al., "Expression of osmotic stress protein 94 in murine endolymphatic hydrops model," *Acta Otolaryngol.* **132**(Suppl. 1), S118–S123 (2012).
14. M. Takumida, N. Akagi, and M. Anniko, "A new animal model for Meniere's disease," *Acta Otolaryngol.* **128**(3), 263–271 (2008).
15. R. S. Kimura, "Animal models of endolymphatic hydrops," *Am. J. Otolaryngol.* **3**(6), 447–451 (1982).
16. E. A. Dunnebier et al., "Two-phase endolymphatic hydrops: a new dynamic guinea pig model," *Acta Otolaryngol.* **117**(1), 13–19 (1997).
17. Y. Tona et al., "In vivo imaging of mouse cochlea by optical coherence tomography," *Otol. Neurotol.* **35**(2), e84–e89 (2014).
18. C. A. Megerian et al., "Surgical induction of endolymphatic hydrops by obliteration of the endolymphatic duct," *J. Vis. Exp.* **35** (2010).
19. B. Bouma et al., "High-resolution optical coherence tomographic imaging using a mode-locked Ti-Al_2O_3 laser source," *Opt. Lett.* **20**(13), 1486–1488 (1995).
20. J. C. Andrews and A. Bohmer, "The surgical approach to the endolymphatic sac and the cochlear aqueduct in the guinea pig," *Am. J. Otolaryngol.* **10**(1), 61–66 (1989).
21. S. S. Gao et al., "In vivo vibrometry inside the apex of the mouse cochlea using spectral domain optical coherence tomography," *Biomed. Opt. Express* **4**(2), 230–240 (2013).
22. B. J. Wong et al., "Optical coherence tomography of the rat cochlea," *J. Biomed. Opt.* **5**(4), 367–370 (2000).
23. S. S. Gao et al., "Quantitative imaging of cochlear soft tissues in wild-type and hearing-impaired transgenic mice by spectral domain optical coherence tomography," *Opt. Express* **19**(16), 15415–15428 (2011).
24. T. Yamasoba and K. Kondo, "Supporting cell proliferation after hair cell injury in mature guinea pig cochlea in vivo," *Cell Tissue Res.* **325**(1), 23–31 (2006).
25. Y. Terayama et al., "Ultrastructural changes of the nerve elements following disruption of the organ of Corti. I. Nerve elements in the organ of Corti," *Acta Otolaryngol.* **83**(1-6), 291–302 (1977).

Nam Hyun Cho received his PhD degree in electronics engineering from Kyungpook National University, Republic of Korea. He is now a researcher in the Center for Soft and Living Matter at the Institute for Basic Science. His research is focused on biomedical imaging, optical imaging for medical, and biological applications.

Jang Woo Lee is a PhD candidate in electronics engineering from Kyungpook National University, Republic of Korea. He is now a researcher in the Institute of Biomedical Engineering Research. His main interests include fully implantable middle ear hearing device and bio-signal measurement.

Jin-ho Cho, PhD, is a professor of the School of Electronics Engineering, Kyungpook National University, Republic of Korea. He is now a director of the Institute of Biomedical Engineering Research in Kyungpook National University. His research is focused on development of totally implantable middle ear hearing device for the human hearing loss patients.

Jeehyun Kim, PhD, is an associate professor of electronics engineering from Kyungpook National University, Republic of Korea. His research interests and expertise include optical imaging for biomedical application.

Jeong Hun Jang, PhD, is an assistant professor in otorhinolaryngology at Kyungpook National University College of Medicine. His research is focused on using optical coherence/Doppler tomography for middle/inner ear pathological imaging and clinical data analysis.

Woonggyu Jung, PhD, is an assistant professor of the School of Nano-Bioscience and Chemical Engineering at Ulsan National Institute of Science and Technology, Republic of Korea. He is now a professor in the Center for Soft and Living Matter at the Institute for Basic Science. His research is focused on biomedical optics, and optical imaging for neuroscience applications.